



Research Article

Design of an efficient laser diode driver with single stage power factor correction

Ahmet Yiğit SARI^{1,*}, Ali Rifat BOYNUEĞRİ^{1,2}

¹Department of Electrical Engineering, Yıldız Technical University, Istanbul, Türkiye

²Clean Energy Technologies Institute, Yıldız Technical University, Istanbul, Türkiye

ARTICLE INFO

Article history

Received: 27 April 2024

Accepted: 31 May 2024

Key words:

Laser Diode Driver; Laser Power; LLC Resonant Converter; Transmission; Power Factor Correction; Transmission; Wireless Power.

ABSTRACT

Laser power transmission (LPT) has emerged as an innovative technology revolutionizing long-distance wireless power delivery. The efficiency of an LPT system significantly relies on the performance of the laser diode (LD) driver. This paper introduces an innovative single-stage AC-DC LLC converter with power factor correction (PFC) designed for LD drivers, addressing the specific demands of LDs. The proposed system achieves exceptional operational metrics, including high efficiency and minimal harmonic distortion in the input current. Through meticulous design and evaluation, the system demonstrates its capability to meet the intricate demands of LDs while maintaining minimal current ripple, marking a significant advancement in LPT technology. Furthermore, this study underscores the importance of LD driver efficiency by showcasing a single-stage AC-DC LLC with PFC converter that achieves an outstanding efficiency of 95.44% alongside a minimal current total harmonic distortion (THD) of 2.53%. This research represents a pivotal step toward enhancing LD driver efficiency within the domain of LPT, promising extensive applications in wireless power transmission

Cite this article as: Sarı AY, Boynueğri AR. Design of an efficient laser diode driver with single stage power factor correction. Clean Energy Technol J 2024;4:1:1-7.

INTRODUCTION

In recent years, Wireless Power Transmission (WPT) technology has experienced notable advancements, facilitating the transfer of energy without the necessity for physical or electrical interconnections between two points [1,2]. This technology has garnered significant interest in both industrial applications and consumer electronics. Compared to traditional power transmission methods, Wireless Power Transfer (WPT) offers numerous advantages such as reliability, durability, aesthetic design, originality, and ease of use. Consequently, WPT technology has begun to be utilized in a wide range of applications, from mobile devices to electric vehicles [3-5].

Highlights

- Enhances efficiency with ZVS
- Ensures 2.53% current THD
- Single-stage configuration eliminates extra switches
- Meets specific voltage and current requirements of laser diode accurately

Various methodologies exist for WPT, encompassing inductive power transfer, capacitive power transfer, microwave power transfer, and laser power transmission (LPT) [6-8]. LPT technology emerges as a promising choice for WPT, especially in the context of mobile devices like un-

*Corresponding author:

*E-mail address: yigit.sari@yildiz.edu.tr



manned aerial vehicles and robots [9]. This technology enables uninterrupted power transfer over considerable distances, spanning several kilometers, facilitated by a high-power density laser beam [10,11].

At recent studies, laser diode (LD) has become crucial for LPT applications. Their efficiency and compact design have made them a favoured option in the field of LPT. One of the most critical challenges for LPT is the efficiency of LD [12]. The LD driver circuit plays a crucial role within the system, impacting both laser performance and overall system efficiency [13]. In LD driver circuits, linear current regulators are commonly preferred [14]. However, this method results in efficiency losses. Buck and boost converters, widely used topologies, offer an effective solution to this efficiency challenge. To meet LD requirements, researchers have driven the LD by connecting a buck converter, providing the DC component of the current, in parallel with a bidirectional converter, supplying the AC component. They achieved an efficiency of 88% at an average output power of 20 W [13]. Another significant challenge arises from LD being a current-driven device, leading to current ripples. LD demand a stable driving current, and low-ripple current is crucial [15]. A single-stage converter based on an advanced design was utilized, employing an LCL filter to reduce LD current ripples. While the circuit was documented to achieve high efficiency, no specific efficiency value was provided [16]. There are several relevant studies focusing on efficiency and current ripples, all of which primarily concentrate on DC-DC converters. However, there aren't enough studies into an AC-DC LD driver circuit. Since DC-DC converters are used between low voltage differences, different types of converters were chosen, but the LLC operating principle is advantageous in terms of high efficiency and wide input voltage range [17]. The LLC resonant converter features the advantage of zero-voltage switching (ZVS) operation, which enhances conversion efficiency and reduces electromagnetic interference (EMI) [18]. This feature has garnered significant attention in both research and various applications [19-21]. The LLC resonant converter's inherent ability to achieve high voltage gain under light loads and low voltage gain under heavy loads facilitates input current shaping across a wide voltage range [22]. This characteristic aligns with the traits of a PFC converter, emphasizing its significance in power factor correction (PFC) [23]. Consequently,

the LLC resonant converter proves highly suitable for direct single-stage AC-DC conversion [24-25].

In this study, a high-efficiency LLC resonant converter with integrated grid PFC, low current total harmonic distortion (THD), single-stage operation, and ZVS at high powers has been employed to increase system efficiency. The LLC converter operates with a lower voltage, relative to the input voltage, and high current, facilitating soft switching, supplying of LD demands.

System Description

As mentioned above, achieving high efficiency and minimizing current ripple is crucial when driving LD. To supply LD demand, a highly efficient LLC-based isolated single-stage PFC converter is employed. The proposed LD driver circuit diagram is shown in Figure 1.

Proposed LD driver circuit diagram. The driver circuit comprises the input rectifier, input filter, LLC inverter, LLC resonant tank, transformer, output rectifier, and output filter. In the input rectifier section, S1-S4 switches, forming a full bridge configuration, are utilized to ensure synchronous rectification. Implementation of full bridge synchronous rectification instead of a diode bridge significantly reduces conduction loss. At the input filter stage, L_{in} and C_{in} are utilized to filter the rectified input current. At the LLC inverter part Q1-Q4 switches are convert to DC wave to high frequency AC wave and at the suitable operation conditions, ZVS feature achieved by LLC inverter part. Resonant capacitance C_r , resonant inductance L_r , and the transformer's magnetizing inductance L_m together constituting LLC resonant tank. The resonant tank enables the circulation of high-frequency and sinusoidal voltage, enables the transmission of energy to the load through the transformer. At the output rectifier part there are SR1-SR2 switches constitutes full wave rectifier to convert AC voltage to DC voltage. The substitution of a full-wave rectifier in place of a full bridge rectifier results in decreased conduction losses by reducing the required switches from four to two. This implementation is only achievable by utilizing a center-tapped transformer, making the center-tapped transformer the selected component for the circuit. In the output filter section, L_o and C_o are utilized to effectively filter the output current, meeting the specific requirements necessary for supplying the LD demands. The output filter section is crucial due to the specific demands of LD.

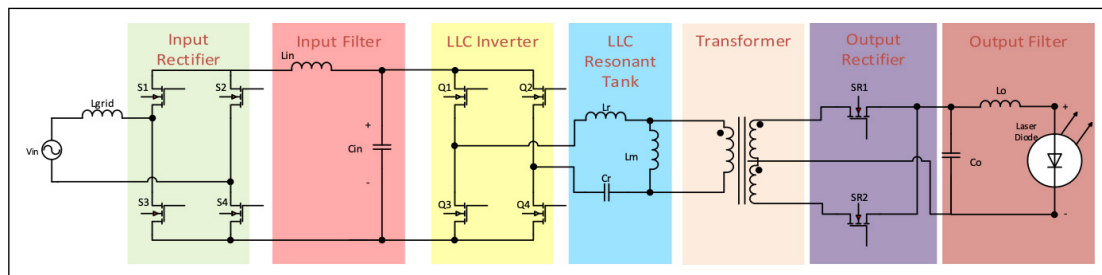


Figure 1. Proposed LD driver circuit diagram.

Calculations

There are three operational region of LLC converter, capacitive, inductive and resistive region. Operating at capacitive, inductive or resistive region is depend on f_s switching frequency and f_p critical resonant frequency, which is formulated at Eq. 1. Additionally, as indicated in Eq. 2, the M value depends on the switching frequency f_s . M represent the voltage gain of the LLC circuit and, together with the conversion ratio of the transformer, determines the ratio of the input voltage to the output voltage. In conjunction with the determination of appropriate frequency range of LLC inverter, the LLC circuit topology significantly reduces switching losses through ZVS and operate at inductive region. If the appropriate frequency range cannot be determined, the LLC circuit operates in the capacitive region, leading to the forfeiture of its ZVS feature and causing switching losses. Consequently, operating in the capacitive region results in an efficiency loss. It is clear that the LLC gain value must change simultaneously with the change of the input voltage. In AC-DC PFC applications, LLC's operating point is continuously altering because of the input voltage's (AC Grid's) characteristic.

$$f_p = \frac{1}{2\pi\sqrt{(L_r + L_m)C_r}} \quad (1)$$

$$M_{LLC, total}(f_s, \theta) = \frac{1}{2n} \cdot \frac{1}{\sqrt{\left[1 + \frac{1}{Y} \left(1 - \frac{f_s^2}{f_p^2}\right)\right]^2 + 4(\sin(\theta))^4 \left[\left(\frac{f_s^2 - f_p^2}{f_s f_r}\right) Q_{full_load}\right]^2}} \quad (2)$$

$$Q_{full_load} = \frac{\pi^2}{8n^2} \cdot \frac{I_{out}}{V_{out}} \sqrt{\frac{L_r}{C_r}} \quad (3)$$

$$f_r = \frac{1}{2\pi\sqrt{L_r C_r}} \quad (4)$$

$$n = \frac{N_p}{N_s} \quad (5)$$

Q is the quality factor as specified in Eq.3, f_r is the resonant frequency as show in Eq. 4, n is the turn ratio of the transformer as indicated in Eq. 5, Y is the ratio of magnetizing inductance L_m to resonant inductance L_r , as expressed in Eq. 6. As depicted in Eq. 2, M varies with θ 's changes because θ represents the phase angle of the input voltage, and this angle undergoes time-dependent variations. As a result, f_s is consistently changing to adjust to meet the load's requirements, adapting despite variations in the phase angle. It is crucial to avoid operating at the capacitive region due to the operational traits of the LLC circuit at capacitive region. Preventing this operation depends on factors such as the gain curve M , f_s , L_m , L_r , and the critical resonant frequency, f_p . Critical resonant frequency f_p is occurring when components L_m , L_r and C_r resonate together, acts as the critical threshold to prevent the LLC circuit from operating at the capacitive region.

$$Y = \frac{L_m}{L_r} \quad (6)$$

$$M_{LLC, total}(f_p, \theta) = \frac{1}{2n} \cdot \frac{1}{\sqrt{\left[1 + \frac{1}{Y} \left(1 - \frac{f_s^2}{f_p^2}\right)\right]^2 + 4(\sin(\theta))^4 \left[\left(\frac{f_s^2 - f_p^2}{f_s f_r}\right) Q_{full_load}\right]^2}} \quad (7)$$

Mis calculated by Eq. 7. The LLC circuit must consistently operate above the specified limit frequency denoted as f_p . If f_s is lower than f_p , ZVS capability becomes non exist. For any value where Q is greater than zero, the M value should exceed the M value that calculated at f_p . To increase efficiency and supplying LD demands, f_s must always be greater than f_p . To meet these conditions, calculating the M value using Eq. 3 and Eq. 7 is essential. Operating within the inductive region guarantees ZVS and ensures high efficiency. When calculating the M value, thorough analysis of the load's electrical characteristics is essential. In this study, the load is LD. Since LD's are current driven devices, they must be carefully analysed and electrical modelling must be carefully done. In this study, LD is modelled as a diode due to its similarities to diodes in terms of electrical parameters, such as having a threshold voltage. It is obvious that when modelling the LD, resistance of the LD must first be calculated by considering electrical parameters of the LD. LD parameters are given in Table 1.

Resistance of LD can be calculating by using Eq. 8. Where R_{on} is resistance of LD, V_{op} is operating voltage of LD, V_{th} is threshold voltage of LD and I_{op} operating current of LD. The LD used in this model operates in continuous wave (CW) mode. In addition to obtaining the demanded current value, as mentioned above, one of the most critical issues of LD is the current ripple, and if low current ripple demand can't be satisfied, the LD will overheat and cannot supply the demanded efficiency. Hence, the value of the output filter should be high, and the PFC controller becomes more complex.

$$R_{on} = \frac{(V_{op} - V_{th})}{I_{op}} \quad (8)$$

Controller

Control diagram of PFC LLC LD Driver Circuits shown in Figure 2. Because of the LD's demands, this controller has differences between common PFC controllers. At common PFC controllers, demanded output voltage of the circuit chosen for PFC controller to get demanded output voltage. But in Figure 2 considering with LD's are current driven devices and current ripples are needed minimized, demanded output current I_{outref} is chosen reference signal of PFC controller to supply LD's demands. PI-1 and PI-2 parameters are given at Table 2.

I_{outref} is demanded output current of the circuit and I_{out} is the output current of the circuit. Reference signal of the circuit is chosen output current instead of output voltage to supply

Table 1. Electrical parameters

Threshold Current (A)	1.7 A
Threshold Voltage (V)	24 V
Operating Current (A)	34.04 A
Operating Voltage (V)	30.1 V

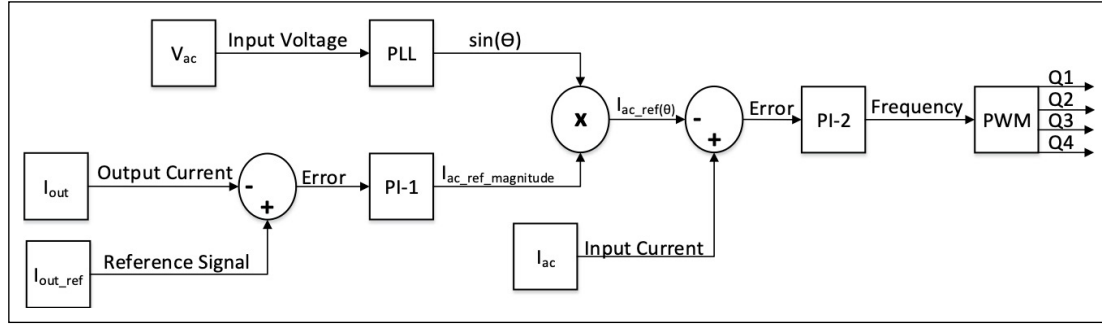


Figure 2. Controller of AC LLC LD driver circuit.

Table 2. PI-1 and PI-2 parameters

PI-1 Parameters	Value	PI-2 Parameters	Value
K_{p1}	0.64706	K_{p2}	2000
K_{i1}	2.22	K_{i2}	500000000

LD's demands. PI-1 is utilized to generate $I_{ac_ref_magnitude}$ and this way output current is regulated. Differences between I_{outref} and I_{out} is the error signal and this signal is the input parameter of PI-1. $I_{ac_ref_magnitude}$ signal is the magnitude of demanded input current. Phase Locked Loop is utilized to get the reference sine signal from input voltage V_{ac} . PLL is generate a reference $\sin(\theta)$ signal that is the same phase and frequency with V_{ac} . $I_{ac_ref_mag-nitude}$ obtained from PI-1 and used for defining the magnitude of the circuit's input current, $\sin(\theta)$ is obtained from PLL and used for demanded pure sine shape of the input current. $I_{ac_ref(\theta)}$ signal is created by multiplying the reference $\sin(\theta)$ signal and magnitude of demanded input current, $I_{ac_ref_magnitude} \cdot I_{ac_ref(\theta)}$ signal is demanded input current. Differences between input current I_{ac} and demanded input current $I_{ac_ref(\theta)}$ is the input of PI-2. PI-2 is utilized to generate appropriate frequency to the Q1-4 switches gates. Owing to this controller, the desired current value and low current ripples, as demanded by the LD, have been successfully achieved.

Simulation Results

The simulation of the Single-stage PFC LLC LD driver is performed using MATLAB Simulink, validating all the theoretical calculations and diagrams mentioned above. A sample time of 42.553 nano seconds and a stop time of 0.8 seconds were employed, resulting in a comprehensive and detailed analysis. electrical input and output parameters are given at Table 3.

As shown in Table 3 parameters of modelling is performed and LD demands are successfully achieved. As mentioned above, for demanded LLC performance, f_s should not be smaller than f_p to operate at inductive region for ensuring ZVS and highly efficiency LLC. As shown in Table 3, 95.44% efficiency has been reached, efficiency value is calculated by using:

$$\eta\% = \frac{P_{out}}{P_{in}} \cdot 100 \quad (9)$$

The decrease in efficiency primarily stems from losses incurred in both active and passive components. Passive component losses arise due to inductance, capacitance, and resistance, whereas active component losses are attributed to switching. Notably, switching losses are minimal in this circuit due to the implementation of ZVS in the LLC inverter section. This feature significantly contributes to the circuit's high efficiency. This situation has been achieved by

Table 3. Electrical parameters

Parameters	Descriptions	Parameters	Descriptions
V_{in}	220 V	L_r	26 μ H
I_{in}	4.88 A	L_m	104 μ H
P_{in}	1074 W	C_r	392nF
V_{out}	30.1 V	n	6.168
I_{out}	34 A	f_s	24kHz-145kHz
P_{out}	1025 W	f_r	50kHz
Efficiency	0.9544	f_p	22.361kHz
f_{grid}	50 Hz	S1-4	600V, $R_{DS(on)}=60m\Omega$
L_{in}	900 μ H	Q1-4 Switches	650 V, $R_{DS(on)}=41m\Omega$
C_{in}	20nF	SR1-2 Switches	60V, $R_{DS(on)}=2m\Omega$
L_{out}	60mH	C_{out}	9mF

appropriate determination of the circuit parameters. L_{in} and C_{in} form the input filter, while L_{out} and C_{out} constitutes the output filter. Output filter is one of the most critical parts of LD driver because of the LD's low current ripple demand.

The frequency values within an input voltage period, as illustrated in Figure 3, are critical for achieving the required M value. Specifically, at points 0.46-0.47 and 0.48, the input voltage reaches zero, resulting in the minimum frequency. Conversely, at points 0.465 and 0.475, the input voltage peaks, leading to the maximum frequency. This relationship between voltage points and frequency is depicted in both Figure 3 and Table 3. To optimize system performance, it's essential to maintain f_s consistently higher than f_p throughout the entire cycle. This practice safeguards the ZVS feature, ensuring enhanced system performance and efficiency.

As depicted in Figure 4, the LD demands of 30.1 V and 34.04 A have been successfully achieved. Achieving near 1% current ripple, attributed to the output filter and PFC controller, significantly enhances LD performance by mitigating overheating issues and ensuring operational efficiency.

As demonstrated in Figure 5(a), the experimental results reveal the attainment of a nearly pure sine wave input current profile, showcasing the effectiveness of the proposed circuit design in achieving smooth and sinusoidal current waveforms. Furthermore, as illustrated in Figure 5(b), the achieved low current Total Harmonic Distortion (THD) value of 2.53% emphasizes the system's ability to mitigate harmonic distortions, further corroborating its ef-

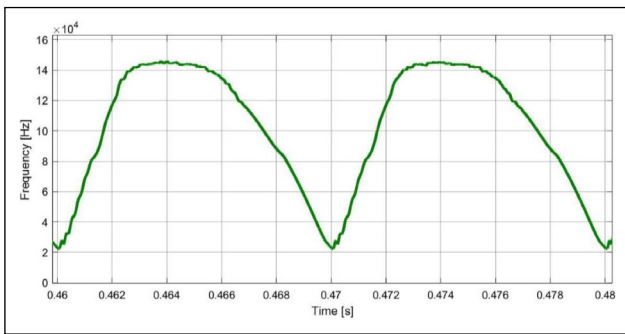


Figure 3. Frequency modulation.

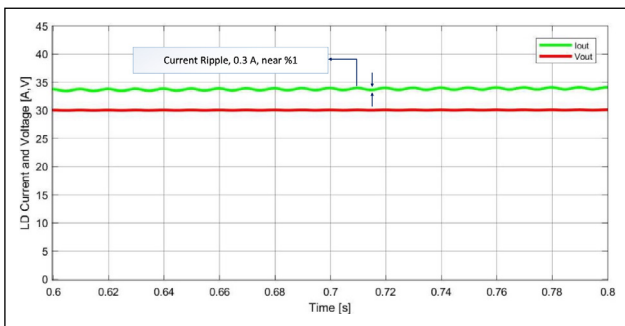


Figure 4. LD current and voltage.

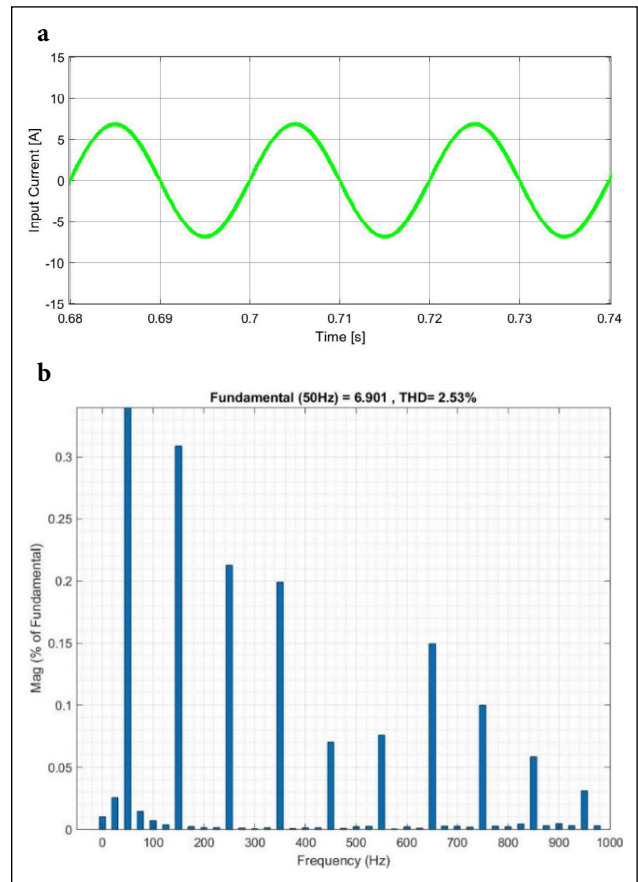


Figure 5. Input current and THD values.

ficient performance. The notable reduction in THD levels signifies the efficacy of the Power Factor Correction (PFC) controller in regulating the input current waveform, thereby ensuring enhanced power quality and reduced electrical noise. These findings highlight the successful implementation of the proposed approach, resulting in minimized input current ripple and the generation of a near-ideal sinusoidal output.

CONCLUSION

In this study, a substantial contribution has been made toward enhancing the efficiency of LD driver systems with in LPT technology. Compared to other laser drivers mentioned in the literature, the designed laser driver offers high power and efficiency. In contrast to other grid-connected circuit topologies, it is single-stage and highly efficient as it eliminates the need for an additional switch. However, its controller presents challenges in implementation. The pivotal integration of a robust and efficient LLC resonant converter, incorporating functionalities like PFC, grid integration, and ZVS, stands out. The exceptional achievement of 95.44% efficiency and remarkably low current THD at 2.53% accentuates the effectiveness of the proposed approach. Moreover, meeting precise LD demand specifica-

tions, encompassing specific voltage and current requirements with minimal current ripple, further solidifies the applicability of this system within LPT domains. Consequently, this research promises substantial advancements in enhancing LD driver circuit efficiency and performance in the domain of LPT.

Future studies will focus on the suitability and efficiency of AC-DC PFC circuits for LD driving.

ACKNOWLEDGEMENT

This study was supported by Scientific and Technological Research Council of Turkey (TUBITAK) under the Grant Number 121E564. The authors thank to TUBITAK for their supports.

AUTHORSHIP CONTRIBUTIONS

Authors equally contributed to this work

DATA AVAILABILITY STATEMENT

The authors confirm that the data that supports the findings of this study are available within the article. Raw data that support the finding of this study are available from the corresponding author, upon reasonable request.

CONFLICT OF INTEREST

The author declared no potential conflicts of interest with respect to the research, authorship, and/or publication of this article.

ETHICS

There are no ethical issues with the publication of this manuscript.

REFERENCES

- [1] Jin K, Zhou W. Wireless laser power transmission: A review of recent progress. *IEEE Trans Power Electron* 2019;34:3842–3859.
- [2] Triviño A, González-González JM, Aguado JA. Wireless power transfer technologies applied to electric vehicles: A review. *Energies* 2021;14:1547.
- [3] Xie L, Shi Y, Hou YT, Lou A. Wireless power transfer and applications to sensor networks. *IEEE Wireless Commun* 2013;20:140–145.
- [4] Al-Kalbani AI, Yuce MR, Redouté J-M. A Biosafety Comparison Between Capacitive and Inductive Coupling in Biomedical Implants. *IEEE Antennas Wireless Propag Lett* 2014;13:1168–1171.
- [5] Xu W, Wang X, Li W, Lu C. Research on test and evaluation method of laser wireless power transmission system. *EURASIP J Adv Signal Process* 2022;2022:20.
- [6] He T, Zheng G, Wu Q, Huang H, Wan L, Xu K, et al. Analysis and experiment of laser energy distribution of laser wireless power transmission based on a powersphere receiver. *Photonics* 2023;10:844.
- [7] Dai J, Ludois DC. A survey of wireless power transfer and a critical comparison of inductive and capacitive coupling for small gap applications. *IEEE Trans Power Electron* 2015;30:6017–6029.
- [8] Zhu J, Ban Y, Xu R, Mi CC. An NFC-connected coupler using IPT-CPT-combined wireless charging for metal-cover smartphone applications. *IEEE Trans Power Electron* 2021;36:6323–6338.
- [9] Mason R. Feasibility of laser power transmission to a high-altitude unmanned aerial vehicle. RAND Corporation, Santa Monica, CA, USA. Tech Rep TR-898-AF. 2011.
- [10] Kawashima N, Takeda K. Laser energy transmission for a wireless energy supply to robots. *Proc Symp Automat Robot Construction* 2005;373–380.
- [11] Lim Y, Choi YW, Ryoo J. Study on laser-powered aerial vehicle: Prolong flying time using 976 nm laser source. *Proc Int Conf Inf Commun Technol Converg* 2021;1220–1225.
- [12] Yigit H, Boynuegri AR. Pulsed laser diode based wireless power transmission application: determination of voltage amplitude, frequency, and duty cycle. *IEEE Access* 2023;11:54544–54555.
- [13] Zhou W, Jin K. Efficiency evaluation of laser diode in different driving modes for wireless power transmission. *IEEE Trans Power Electron* 2015;30:6237–6244.
- [14] Thompson MT, Schlecht MF. High power laser diode driver based on power converter technology. *IEEE Trans Power Electron* 1997;12:46–52.
- [15] Chen F-Z, Song Y-C, Ho F-S. An efficiency improvement driver for master oscillator power amplifier pulsed laser systems. *Processes* 2022;10:1197.
- [16] Sharma A, Panwar CB, Arya R. High power pulsed current Laser Diode driver. 2016 International Conference on Electrical Power and Energy Systems (ICEPES), Bhopal, India. 2016;120–126.
- [17] Liu W, Yurek A, Sheng B, Chen Y, Liu Y-F. A single stage 1.65kW AC-DC LLC converter with power factor correction (PFC) for on-board charger (OBC) application. 2020 IEEE Energy Conversion Congress and Exposition (ECCE), Detroit, MI, USA. 2020;4594–4601.
- [18] Qiu Y, Liu W, Fang P, Liu Y-F, Sen P-C. A mathematical guideline for designing an AC-DC LLC converter with PFC. 2018 IEEE Applied Power Electronics Conference and Exposition (APEC), San Antonio, TX, USA. 2018;2001–2008.

- [19] Zeng J, Zhang G, Yu SS, Zhang B. LLC resonant converter topologies and industrial applications — A review. *Chinese J Electr Eng* 2020;6:73–84.
- [20] Lee J-Y, Jeong Y-S, Han B-M. An isolated DC/DC converter using high-frequency unregulated LLC resonant converter for fuel cell applications. *IEEE Trans Ind Electron* 2011;58:2926–2934.
- [21] Fang Z, Cai T, Duan S, Chen C. Optimal design methodology for LLC resonant converter in battery charging applications based on time-weighted average efficiency. *IEEE Trans Power Electron* 2015;30:5469–5483.
- [22] Chen Y, Yang D, Shao S, Zhang J. Optimal Design of LLC-based Isolated Single-Stage PFC Converter. 2022 IEEE International Power Electronics and Application Conference and Exposition (PEAC), Guangzhou, Guangdong, China. 2022;1649–1654.
- [23] Zhou Y, Liu S, Ren J, et al. Design Methodology of LLC Resonant Converters for Single-stage Power Factor Correction Application. *J Electr Eng Technol* 2021;16:2573–2584.
- [24] Luo H, Zang T, Zhao C, Chen S, Zhou Y, Qiu Y, et al. Power boundary controlled single-stage LLC power factor correction converter and its optimal parameter design. *IEEE Trans Ind Electron* 2023;70:12219–12232.
- [25] Forouzesh M, Liu Y-F, Sen PC. A line cycle synchronous rectification strategy based on time-domain analysis for single-stage AC–DC LLC converters. *IEEE Trans Power Electron* 2023;38:5077–5091.